Title
Experimental study of flow instabilities in a rotating annulus with local convective forcing

Permalink
https://escholarship.org/uc/item/4hg9p6rw

Journal
International Symposium on Stratified Flows, 1(1)

Authors
Scolan, Hélène
Read, Peter

Publication Date
2016-08-29

Experimental study of flow instabilities in a rotating annulus with local convective forcing.

Hélène Scolan and Peter Read

Department of Physics, Atmospheric, Oceanic & Planetary Physics,
University of Oxford, UK
helene.scolan@physics.ox.ac.uk, peter.read@physics.ox.ac.uk

Abstract

We present a experimental study of flows in a cylindrical rotating annulus convectively forced by local heating in an annular ring at the bottom near the external wall and via a cooled circular disk near the centre at the top surface of the annulus. This new configuration is a variant of the classical thermally-driven annulus analogue of the atmosphere circulation, in which thermal forcing is applied uniformly on the sidewalls. Two vertically and horizontally displaced heat sources/sinks are arranged so that, in the absence of background rotation, statically unstable Rayleigh-Bénard convection would be induced above the source and beneath the sink, thereby relaxing strong constraints placed on background temperature gradients in previous experimental configurations to better emulate local vigorous convection in the tropics and polar regions whilst also facilitating baroclinic motion in midlatitude regions in the Earth's atmosphere. Regimes of flows are identified, depending upon the rotation rate and strength of differential heating by varying control parameters.

1 Introduction

The circulation of the atmosphere is the result of several physical forcing processes: gravity, rotation, radiative exchanges (incoming sunlight, outgoing thermal infrared radiation), clouds and moisture processes, chemical reactions, interaction with surface topography, boundary processes etc... Although numerical global circulation models solving equations of dynamics, thermodynamics and continuity in 3D on a sphere are capable of reproducing and even predicting many features of the observed atmosphere, their complexity and the need to represent unresolved processes by semi-empirical parameterizations means that insights and understanding of how the real atmosphere works may still be elusive. In this context, laboratory analogues of the dynamics of the atmosphere continue to to help scientists understand fundamental dynamical processes in the atmosphere by providing the possibility of precise, reproducible experiments to test ideas and hypotheses.

In the spirit of this approach, the idealization of the midlatitude atmosphere in the laboratory as a differentially-heated, rotating,cylindrical annulus, originally proposed by Hide, has proved to be a prolific and productive analogue of many features of the atmospheric circulation (Hide, 1958; Fowlis and Hide, 1965; Hide et al., 1977; Read et al., 2014). By combining only the three most essential forcing physical ingredients of the atmosphere i.e gravity, rotation and differential heating, the 'classical' thermally-driven rotating annulus provides an experimental configuration that enables both large-scale overturning circulations and baroclinic instabilities to be studied and explored. It has also proved valuable as a tractable 'test bed' within which to test numerical codes and methods (Harlander et al., 2011; Vincze et al., 2015) as well as to benchmark statistical-dynamical analysis methods in widespread use in meteorology, such as data assimilation (Young and Read, 2013).

The classical annulus configuration, however, has some important limitations as an analogue of the mid-latitude atmosphere, an important aspect of which derives from its use of isothermal vertical boundaries to provide heating and cooling (e.g. see Figure 1). This leads to an intense boundary layer dominated overturning circulation which imposes a strong constraint on the background stratification in the working fluid which limits the possibility for internal instabilities to change this, even at large equilibrated amplitudes. In contrast, in the real atmosphere (see Figure 1 a) and c)), the effective heat source is located mostly on the equator near the ground (through absorption of infrared radiation re-radiated from the surface) while the heat sink is predominantly located in the upper troposphere in the mid-latitudes and polar regions (e.g. see Chan and Nigam, 2009). The resulting circulation spontaneously partitions itself into a convectively unstable/neutral region in the tropics that interacts with a statically stable, baroclinic region at mid-latitudes that, despite being cooled from above, is statically stable.
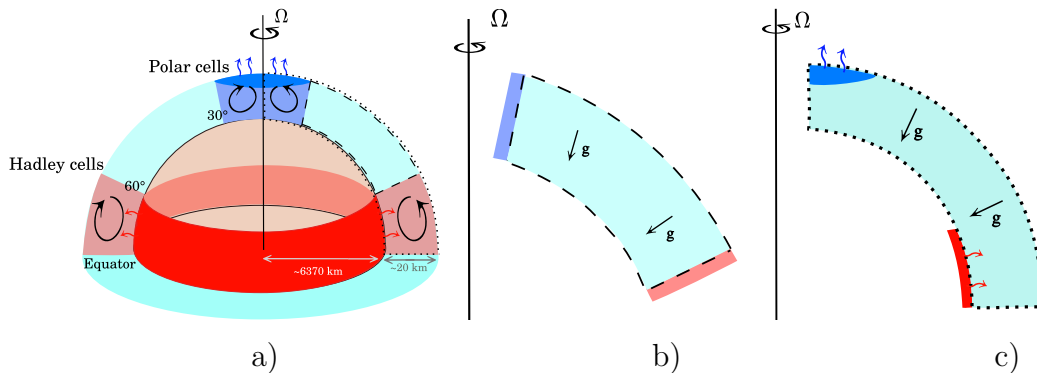

Figure 1: a) Sketch of a simplified structure of the atmosphere and location of the dominant global thermal heat sinks and sources. b) Schematic view of a section of midlatitude atmosphere, as represented b) in the classical annulus and c) in the new annulus analogue, taking into account the heat sink in the upper atmosphere in the polar region and the heat source close to the ground in tropical regions.

Precisely *how* is heat passed from the convectively turbulent region in the tropics into the stably-stratified sub-tropics and mid-latitudes is still not well understood quantitatively. In particular, it is not clear what determines the characteristics of the observed vertical stratification in the midlatitude atmosphere (its static stability, surface thermal contrast, tropopause height) and more generally what are the dominant mechanisms for nonlinear equilibration of baroclinic and convective instabilities in the atmosphere (e.g. see Zurita-Gotor and Lindzen, 2007; Schneider, 2006, for reviews).

In this study, therefore, we have constructed a new laboratory analogue of atmospheric circulation with a rotating annulus that is convectively forced by *local* differential heating. We aim, thereby, to relax some of the thermal constraints on background temperature gradients in the 'classical' annulus experiments in order to to better represent how the thermal structure of the atmosphere itself is maintained, with particular reference to the equilibration mechanisms of convective and baroclinic instabilities. Section 2 describes the characteristics of the experimental setup while some preliminary results are presented in Section 3 and briefly discussed in Section 4.
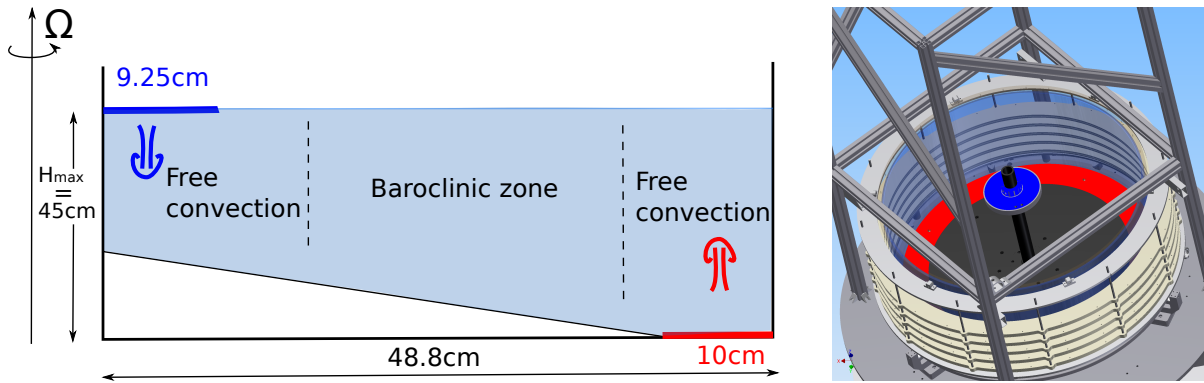
Figure 2: a) Schematic cross-section of half of the new annular experimental setup with local thermal heat source and heat sink horizontally and vertically displaced. b) Zoomed view of the design of the new setup with the electrically heated annular ring at the bottom of the tank in red and the cooling imposed through a circular disk at the centre of the tank at the upper surface in blue (with cold water circulation).

2 Experimental setup

The new experimental configuration is derived from the model illustrated in Figure 1 c). By unwrapping the domain, this leads to the usual atmosphere-like cylindrical configuration, but where local differential heating is used to emulate the local heat sink in the upper atmosphere in polar regions and the heat source near the ground in tropical regions. This allows the formation of a statically stable (though baroclinically unstable) zone, sandwiched between convectively unstable regions over/underlying the heated or cooled boundaries (see also the Wright *et al* paper in this volume presenting results of a companion numerical study of axisymmetric flow 2D regimes) and permits potential feedback of baroclinic instability onto the background stratification.
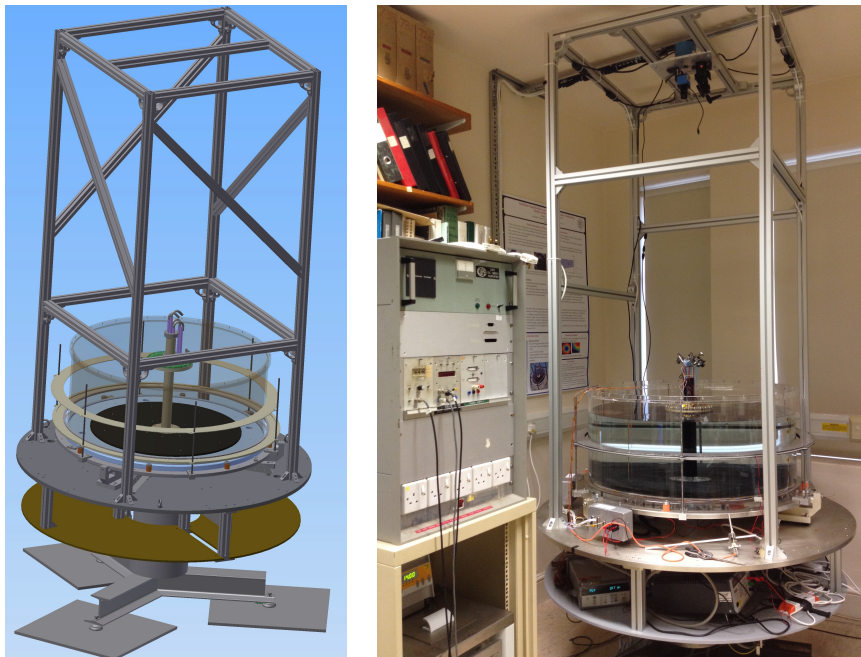

Figure 3: Global view of the experimental setup.

The experiments are carried out in a new circular tank, mounted on a turntable
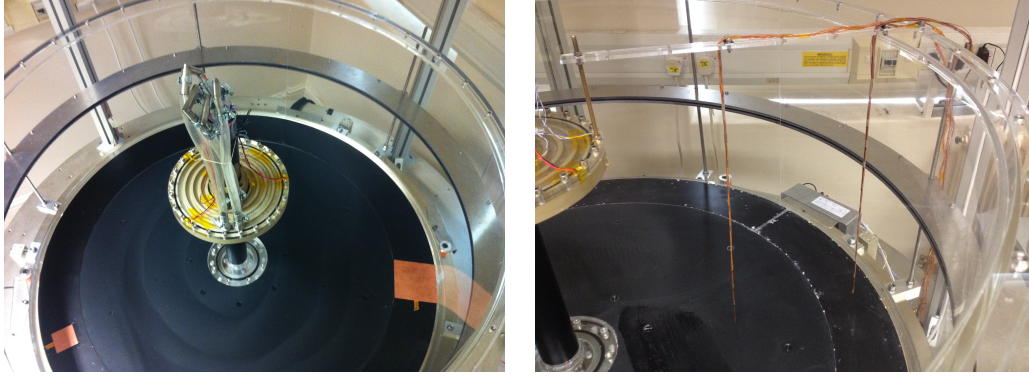
Figure 4: a) Top-view of the experimental setup with instrumented cold plate and aluminium annular ring with Platinum resistance sensors and type T thermocouples and two heat fluxmeters, visible spanning the width of the outer ring. The infill piece at smaller radii at the bottom is made of black perspex. b) 3mm diameter rods instrumented with ten type T microthermocouples to measure thermal stratification above the statically stable zone at mid-radius and above the heated external zone.

rotating in an anticlockwise direction at angular velocity Ω up to $3.5 \, \mathrm{rad/s}$. The global design and a view of the whole assembly of the new experimental setup is presented in figure 3: it shows the perspex tank of internal radius $b = 48.8 \, \mathrm{cm}$ filled with water and including a cooled circular disk of radius $9.25 \, \mathrm{cm}$ attached to a central $5 \, \mathrm{cm}$ diameter cylindrical post (i.e with inner annulus radius a=$2.5 \, \mathrm{cm}$) cooled with water circulated from an external water bath in the lab frame via a rotary union (see figure 5) and with top-view cameras attached to the rotating aluminium framework. The 10 cm wide, electrically heated, annular ring is composed of two aluminium plates onto which flexible plastic-coated heaters are attached (see figure 4 for a closer view and details in figure 5). Both the cold plate and the electrically heated annular plate are equipped with heat fluxmeters and thermal probes (see figure 4) with watertight wire connections at the bottom of the tank (Figure 5). As visible in the close-in view in Figure 4, an annular silver ring is located around the tank and consists of a series of LED arrays, generating a sheet of white light collimated between two thin, aluminium plates to produce a 5–10 mm thick horizontal light sheet (see Figure 5 at the right hand side). On the shelf underneath the main turntable are located a remotely controlled computer, the acquisition system for the thermal probes (multiplexer) and power supplies for the lights and for the heaters fixed on the annular ring.

In common with the conventional rotating annulus experiment, the principal dimensionless parameters expected to govern the behaviour of the system are the thermal Rossby number, a stability parameter comparing the Rossby deformation radius to $L = b - a$ the horizontal size of the tank,

$$\Theta = \frac{g\rho_1 \Delta T H}{\Omega^2 L^2}, \tag{1}$$

the Ekman number, comparing viscous and rotation effects,

$$E = \frac{\nu}{\Omega H^2}, \tag{2}$$

which can be rewritten in terms of the historical Taylor number,

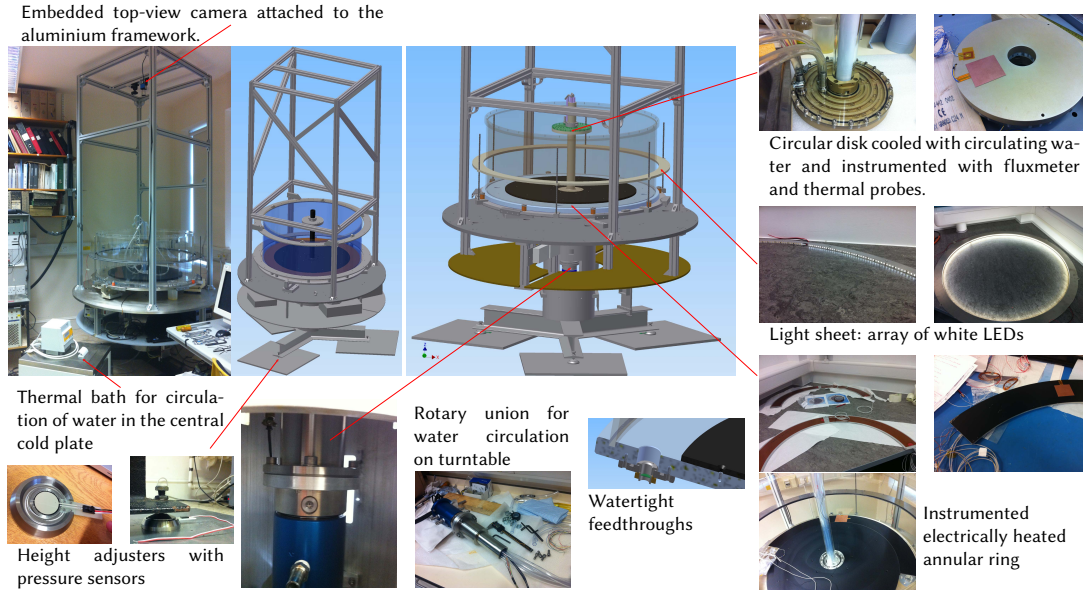$$Ta = \frac{4\Omega^2 L^5}{h\nu^2}. \tag{3}$$

Figure 5: Details of the different elements of the new experimental setup.

Other intrinsic parameters are determined once geometry and working fluid are chosen: the aspect ratio $\Gamma = \frac{L}{H}$ and the Prandtl number $\sigma = \frac{\nu}{\kappa}$ which compares viscous and thermal diffusivities.

Some initial experiments have been carried out with a $30\,\mathrm{cm}$ depth of water ($\sigma \approx 7$) or a mixed solution of water and 17% glycerol ($\sigma \approx 13$) in the current flat-bottomed tank, rotating at $\Omega = 0.03$–$1.1\,\mathrm{rad/s}$. The two heaters are powered such that a maximum power of 206W is injected via the heated annulus while the command temperature of the bath for the water circulation is set to $14\,^{\circ}\mathrm{C}$ and air-conditioning is set to $21\,^{\circ}\mathrm{C}$ in the room. This leads to a maximum effective $\Delta T \approx 7$–$9\,^{\circ}\mathrm{C}$ between the cold plate and the aluminium annular ring, consistent with a measured total power from the heated ring and into the cold plate of around 130 and 60 W respectively. After the first day or two of equilibration, changes in rotating rate were carried out and the system was allowed to relax to a new equilibrated dynamical regime for one hour or more and thermally monitored before image acquisition. The range of values for Θ and Ta in the experiments can be retrieved from the diagram in Figure 9.

In experiments using pure water, an exploration of the different regimes was performed by injecting a concentrated solution of fluoresceine dye to highlight vortices and other flow features, while in the water-glycerol experiments, 355–500 μm Pliolite particles matching the density of the solution (≈ 1.043) were suspended in the fluid and illuminated by the LED light sheet to trace the flow. Images were acquired with a DFK 31BF03 *Imaging Source* firewire camera (resolution 1024×768) and an ethernet AVT Manta 609B camera (resolution 2752×2206) at a frame rate of 1 fps embedded in the rotating frame. In experiments with particles, streaklines were produced by superposing 50 images together in a given equilibrated regime. In addition, an FLIR i50 thermal imaging camera (resolution 240×320) was used to image the temperature variations across the surface of the water.

3 Results

In the range of rotation rates and difference of temperature used, it was expected that the isopycnals in the statically stable region near mid-radius would be quite strongly sloping

(see Wright et al in preparation and the report by Wright et al. in this current volume presenting companion numerical work) such that baroclinic instabilities would be able to grow. Figure 6 shows examples of typical observations of flow patterns found in the fluid, illustrated with dye passive tracer images and infrared camera images. Indeed, several modes of baroclinic instability were observed, as illustrated in figure 7, from low-order regular azimuthal wave modes at small angular velocities to irregular and turbulent motions with small, chaotic vortices at higher rotation rates. In the same way, Figure 8 shows an example of oscillations that can be seen in the outputs of the central thermal probe associated with baroclinic motion for a rotating rate of $0.12\,\mathrm{rad/s}$. Figure 6 shows the location of the different observed modes in a Ta-Θ diagram on which dynamical regimes areas from the previous classical, thermally-driven configuration are superimposed. This indicates a reasonably good agreement in the regions of different wave regimes between the new locally forced atmosphere-like configuration compared to the classic rotating annulus case.

Figure 6: Examples of a baroclinic mode 1 (left hand side) and a baroclinic mode 4 (3 panels at the right) visualised via dye experiments and confirmed in infrared camera images.
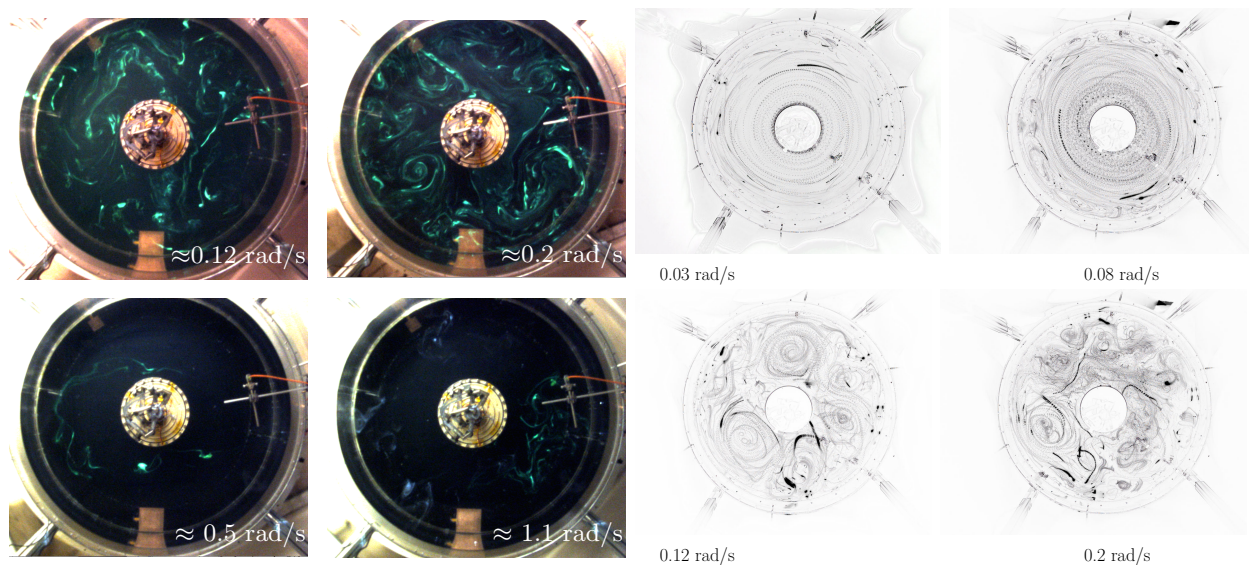

Figure 7: Illustration of the different dynamical regimes of baroclinic instability depending upon the rotation rate. Flow is visualised with fluoresceine or particle streak lines.
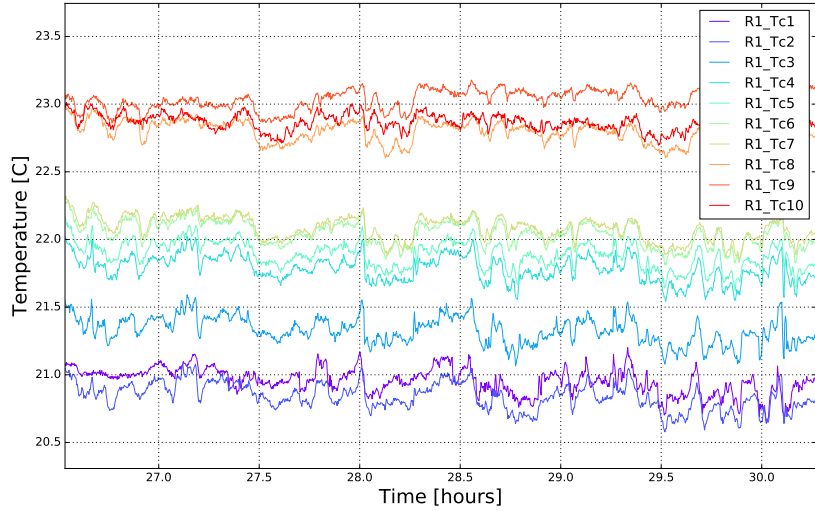
Figure 8: Examples of outputs of the ten thermocouples for the probe located in the mid-radius statically stable baroclinic zone for a rotating rate of 0.12 rad/s.
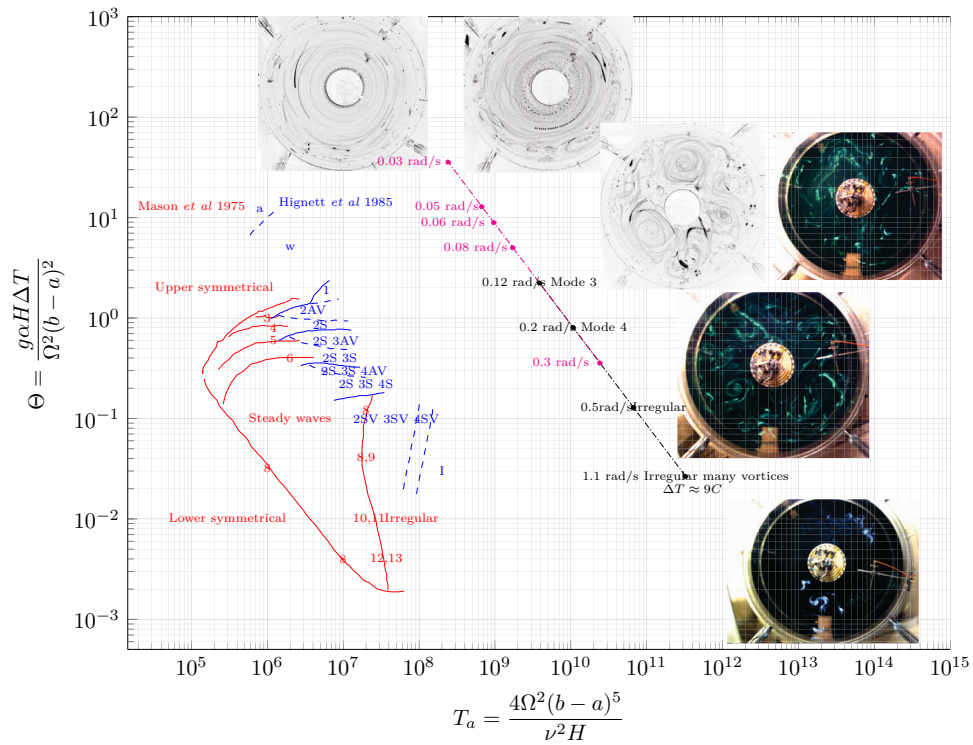

Figure 9: Regime diagram as a function of Taylor number and thermal Rossby number. Black and magenta points show the experimental dynamical regimes explored. Previous results from Mason (1975) and Hignett et al. (1985) in red and blue lines have been plotted for comparison.

4   Conclusion

A new atmosphere-like experiment has been designed in the form of a local convectively forced, thermally-driven, wide rotating annulus to emulate the distribution of local heat sink in the upper atmosphere of the Earth in the polar regions and a heat source near

the ground associated with convection events in tropical regions. The first experiments with this new setup validate the occurrence of baroclinic instability, in agreement with previous results in the classical annular configuration. Further work will include a sloping bottom to take into account in the laboratory effects due to lateralvariations of the Coriolis parameter. Particle image velocimetry experiments will also then allow us to give quantitative insights into the nonlinear baroclinic equlibration processes to help understand the peculiar characteristics and dynamics of a mid-latitude Earth-like atmosphere.

References

Chan, S. C. and Nigam, S. (2009). Residual diagnosis of diabatic heating from era-40 and ncep reanalyses: Intercomparisons with trmm. *Journal of Climate*, 22(2):414–428.

Fowlis, W. and Hide, R. (1965). Thermal convection in a rotating annulus of liquid: effect of viscosity on the transition between axisymmetric and non-axisymmetric flow regimes. *Journal of the Atmospheric Sciences*, 22(5):541–558.

Harlander, U., von Larcher, T., Wang, Y., and Egbers, C. (2011). Piv-and ldv-measurements of baroclinic wave interactions in a thermally driven rotating annulus. *Experiments in fluids*, 51(1):37–49.

Hide, R. (1958). An experimental study of thermal convection in a rotating liquid. *Philosophical Transactions of the Royal Society of London A: Mathematical, Physical and Engineering Sciences*, 250(983):441–478.

Hide, R., Mason, P., and Plumb, R. (1977). Thermal convection in a rotating fluid subject to a horizontal temperature gradient: spatial and temporal characteristics of fully developed baroclinic waves. *Journal of the Atmospheric Sciences*, 34(6):930–950.

Hignett, B. P., White, A., Carter, R., Jackson, W., and Small, R. (1985). A comparison of laboratory measurements and numerical simulations of baroclinic wave flows in a rotating cylindrical annulus. *Quarterly Journal of the Royal Meteorological Society*, 111(467):131–154.

Mason, P. (1975). Baroclinic waves in a container with sloping end walls. *Philosophical Transactions of the Royal Society of London A: Mathematical, Physical and Engineering Sciences*, 278(1284):397–445.

Read, P. L., Prez, E. P., Moroz, I. M., and Young, R. M. B. (2014). *General Circulation of Planetary Atmospheres*, pages 7–44. John Wiley & Sons, Inc.

Schneider, T. (2006). The general circulation of the atmosphere. *Annu. Rev. Earth Planet. Sci.*, 34:655–688.

Vincze, M., Borchert, S., Achatz, U., von Larcher, T., Baumann, M., Liersch, C., Remmler, S., Beck, T., Alexandrov, K. D., Egbers, C., Fröhlich, J., Heuveline, V., Hickel, S., and Harlander, U. (2015). Benchmarking in a rotating annulus: a comparative experimental and numerical study of baroclinic wave dynamics. *Meteorologische Zeitschrift*, 23(6):611–635.

Young, R. and Read, P. (2013). Data assimilation in the laboratory using a rotating annulus experiment. *Quarterly Journal of the Royal Meteorological Society*, 139(675):1488–1504.

Zurita-Gotor, P. and Lindzen, R. S. (2007). Theories of baroclinic adjustment and eddy equilibration.